Dermacozines, a new phenazine family from deep-sea dermacocci isolated from a Mariana Trench sediment†

Wael M. Abdel-Mageed,[a,b] Bruce F. Milne,[c] Marcell Wagner,[d] Marc Schumacher,[e] Peter Sandor,[f] Wasu Pathom-aree,[g] Michael Goodfellow,[g] Alan T. Bull,[h] Koki Horikoshi,[i] Rainer Ebel,[a] Marc Diederich,[e] Hans-Peter Fiedler[d] and Marcel Jaspars*[a]

Received 21st January 2010, Accepted 22nd February 2010
First published as an Advance Article on the web 18th March 2010
DOI: 10.1039/c001445a

Dermacoccus abyssi sp. nov., strains MT1.1 and MT1.2 are actinomycetes isolated from Mariana Trench sediment at a depth of 10 898 m. Fermentation using ISP2 and 410 media, respectively, lead to production of seven new oxidized and reduced phenazine-type pigments, dermacozines A–G (**1–7**), together with the known phenazine-1-carboxylic acid (**8**) and phenazine-1,6-dicarboxylic acid (**9**). Extensive use was made of 1D and 2D-NMR data, and high resolution MS to determine the structures of the compounds. To confirm the structure of the most complex pentacyclic analogue (**5**) we made use of electronic structure calculations to compare experimental and theoretical UV-Vis spectra, which confirmed a novel structural class of phenazine derivatives, the dermacozines. The absolute stereochemistry of dermacozine D (**4**) was determined as *S* by a combination of CD spectroscopy and electronic structure calculations. Dermacozines F (**6**) and G (**7**) exhibited moderate cytotoxic activity against leukaemia cell line K562 with IC_{50} values of 9 and 7 μM, respectively, while the highest radical scavenger activity was observed for dermacozine C (**3**) with an IC_{50} value of 8.4 μM.

Introduction

Marine microbes are uniquely important to life as we know it. Since life most likely began in the oceans, marine microorganisms may be the closest living descendants of the original life forms. Their metabolic diversity and capability allow them to carry out many steps in biogeochemical cycles that other organisms are unable to complete, while on the other hand they are used in a number of biotechnological applications, including the manufacture of industrial products.[1–3] Marine microbes, in particular members of the order *Actinomycetales*, are excellent sources of novel bioactive metabolites with potential pharmaceutical application.[4,5] However, the frequency of rediscovery of known compounds from actinomycetes (one of the major orders of the *Actinobacteria*) is high, and in an effort to isolate novel natural products, the use of so-called "rare" actinomycetes, which have been taxonomically dereplicated, is desirable.[6]

We report here on the chemistry of actinomycetes recovered from sediments collected from the deepest region of the world's oceans, namely the Mariana Trench in the western Pacific Ocean, within which the Challenger Deep, at its southernmost end, is the deepest point on Earth (its depth is variously reported to be 10 915 to 10 920 m).[7] Previously, thirty-eight novel actinomycetes were isolated from deep oceanic sediments, which are considered a promising source of unexplored and new chemical diversity for drug discovery.[4,6,8–10] In our chemical screening program for new metabolites we found that *Dermacoccus abyssi* strain MT1.1, a piezotolerant actinobacterium, and *Dermacoccus* sp. MT1.2 are prolific sources of highly pigmented aromatic compounds, which stimulated our interest in identifying their structures and evaluating their biological activity.

Results and discussion

Dermacoccus abyssi strain MT1.1 was grown in 250 mL baffled shake flasks containing 70 mL of yeast extract-malt extract broth[11] in the presence of HP20 resin for 7 days at a temperature of 28 °C, after first-stage seeding in 10 mL of glucose-yeast-extract[12] upon which cell mass and resin were collected by centrifugation and then extracted with MeOH. Preliminary analysis by HPLC exhibited the presence of several major peaks of highly pigmented aromatic compounds (A, B and D–G) that were isolated subsequently *via* solvent partitioning and chromatography. Maximum production of dermacozines occurred between 96 and 144 h and a 15 L fermentation yielded after purification 49.5 mg of **1**, 12.9 mg of **2**,

[a]*Marine Biodiscovery Centre, Department of Chemistry, University of Aberdeen, Old Aberdeen, Scotland, UK AB24 3UE. E-mail: m.jaspars@abdn.ac.uk; Fax: +44 1224 272921; Tel: +44 1224 272895*
[b]*Department of Pharmacognosy, Faculty of Pharmacy, Assiut University, Assiut, Egypt*
[c]*Center for Computational Physics, Physics Department, University of Coimbra, Rua Larga, 3004-516, Coimbra, Portugal*
[d]*Mikrobiologisches Institut, Universität Tübingen Auf der Morgenstelle 28, D-72076, Tübingen, Germany*
[e]*Laboratoire de Biologie Moléulaire et Cellulaire du Cancer, Hôpital Kirchberg, 9 rue Edward Steichen, L-2540, Luxembourg, Grand-Duchy of Luxembourg*
[f]*Varian Deutschland GmbH, Alsfelder Strasse 6, 64289 Darmstadt, Germany*
[g]*School of Biology, University of Newcastle, Ridley Building, Newcastle upon Tyne, UK NE1 7RU*
[h]*Department of Biosciences, University of Kent, Canterbury, Kent, UK CT2 7NJ*
[i]*Extremobiosphere Research Center, Japan Agency for Marine-Earth Science and Technology, 2-15 Natsushima-cho, Yokosuka, 237-0061, Japan*
† Electronic supplementary information (ESI) available: NMR, UV and mass spectra. See DOI: 10.1039/c001445a

17.4 mg of **4**, 31.2 mg of **5**, 8.5 mg of **6** and 1.6 mg of **7**, which were subsequently used for characterization by spectroscopic methods.

Dermacoccus abyssi strain MT 1.2 was cultivated in a complex medium in 500 mL Erlenmeyer flasks with one baffle because of its strong foaming properties which occurred in aerated stirred-tank fermentors. A crude extract of the culture filtrate was screened by using the HPLC-DAD method described previously.[13] Several major peaks were detected in the HPLC chromatogram, and the lack of UV-visible spectral identity among the 867 reference compounds stored in our HPLC-UV-Vis database prompted us to undertake more detailed investigations in the production behaviour of the strain, and in isolation and structure elucidation of the metabolites. The production of dermacozines started at 48 h, reaching a maximal yield of 5.5 mg L^{-1} after an incubation period of 144 h in the case of dermacozine C, which was the dominant phenazine metabolite produced by strain MT 1.2. Dermacozines were isolated from the culture filtrate (8.5 L) by Amberlite XAD-16 chromatography and subsequently purified by a succession of selective chromatographic steps. Dermacozines C (**3**) and F (**6**) were obtained as orange and blue powders, respectively after lyophilization in amounts of 13 and 7 mg together with known phenazine-1-carboxylic acid (**8**) and phenazine-1,6-dicarboxylic acid (**9**).

Dermacozine A (**1**) was obtained as fluorescent yellowish green powder. The molecular formula was established as $C_{15}H_{14}N_4O_2$ by HRESIMS measurement, thus implying 11 degrees of unsaturation. The IR spectrum of **1** suggested an amide NH_2 (3359, 3328 cm^{-1}) and carbonyl groups (1681, 1673 cm^{-1}). The UV/Vis spectrum showed absorption maxima at 398, 270 (sh), 254 and 208 nm.

The ^1H and ^{13}C NMR spectra in combination with ^1H–^{13}C HSQC NMR data (Tables 1 and 2) of **1** exhibited signals of one methyl group CH_3-15 (δ_H 2.88), six aromatic methines in two 1,2,3-trisubstituted aromatic spin systems [H-2, H-3 and H-4, δ_H 6.96 (d, 8.0), 6.46 (t, 8.0) and 6.30 (d, 8.0); H-7, H-8 and H-9, δ_H 6.56 (d, 8.0), 6.48 (t, 8.0) and 6.30 (d, 8.0)]. In addition, eight quaternary carbon atoms comprising two carbonyls C-13, C-11 (δ_C 171.2 and 171.1 ppm), four nitrogenated C-4a, C-5a, C-9a and C-10a (δ_C 138.8, 133.8, 138.0 and 140.6 ppm), and two olefinic C-1 and C-6 (δ_C 112.3 and 124.5 ppm) moieties were observed. Five hydrogen resonances lacked correlations in the HSQC spectrum of **1** and were therefore recognized as being located on heteroatoms that were identified later as nitrogenous protons for NH_2-12 (δ_H 7.69, 7.28), NH_2-14 (δ_H 7.85, 7.28) and NH-10 (δ_H 9.89).

A database search[14,15] using information from combined 1D and 2D-NMR data indicated the likelihood of a phenazine skeleton being present. Two spin systems and substructures were established by interpretation of the COSY spectrum (Fig. 1a). The connection between these substructures was established using ^1H–^{13}C HMBC correlations (ESI, Table S1†). Thus, correlations from H-3 to C-1, from H-2 to C-11, as well as from H-7 to C-13, and from NH_2-14 and H-8 to C-6, clearly defined the positions of the two amide groups. Correlations from H-4 to C-2 (δ_C 121.2), and from H-9 to C-7 (δ_C 122.5) confirmed the olefinic spin systems H-2, H-3 and H-4 as well as H-7, H-8 and H-9, respectively. Moreover, correlations from H-2 and H-4 to C-10a and from H-3 to C-4a allowed the assignment C-10a and C-4a while HMBC correlations from H-7, H-9 to C-5a and H-8 to C-9a secured the positions of C-5a and C-9a. Furthermore, HMBC correlations from CH_3-15 and NH-10 to C-4a and C-5a defined the position of *N*-methyl group relative to C-4a and C-5a and confirmed the reduced phenazine skeleton.

Dermacozine B (**2**) was obtained as reddish brown powder. High-resolution mass spectrometry gave a molecular formula of $C_{22}H_{18}N_4O_3$, which required 16 degrees of unsaturation. The IR absorption peaks suggested NH_2 (3344, 3214 cm^{-1}) and carbonyl

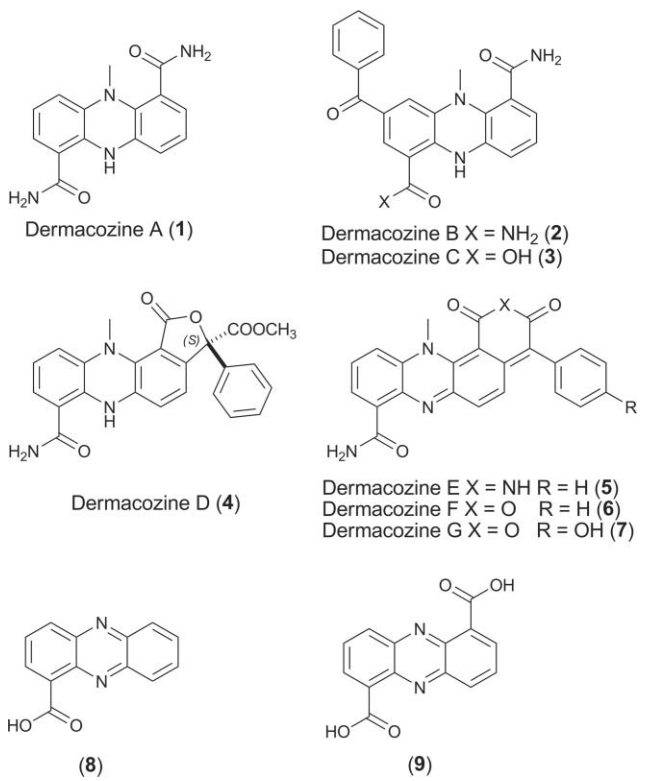

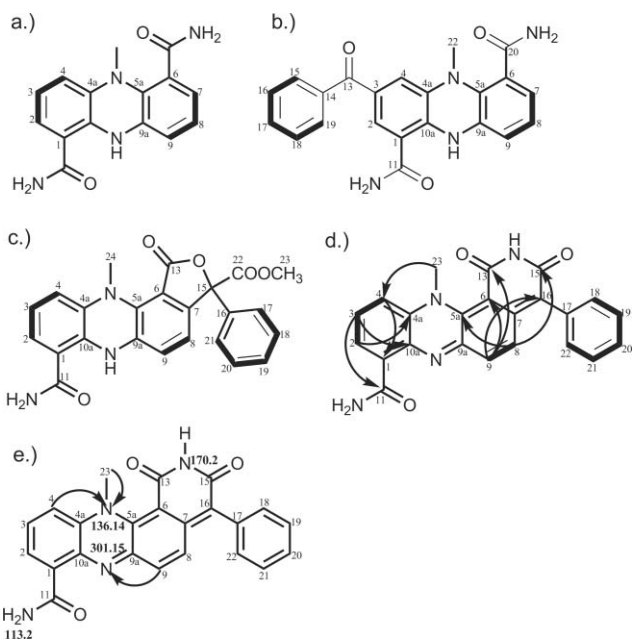

Fig. 1 (a)–(c) Observed COSY correlations (bold bonds) for **1**, **2**, **4**. (d) COSY and long range HMBC (H → C) correlations for **5**. (e) ^{15}N NMR data for **5** (H → N).

Table 1 ^{1}H NMR (400 MHz) data of dermacozines A–D (**1–4**)

No.	**1**[a] δ^{1}H/ppm, mult, J/Hz	**2**[a] δ^{1}H/ppm, mult, J/Hz	**2**[b] δ^{1}H/ppm, mult, J/Hz	**3**[a] δ^{1}H/ppm, mult, J/Hz	**3**[b] δ^{1}H/ppm, mult, J/Hz	**4**[a] δ^{1}H/ppm, mult, J/Hz	**4**[c] δ^{1}H/ppm, mult, J/Hz
1							
2	6.96 (1H, d, 8.0)	7.43 (1H, brs)	7.43 (1H, d, 2.0)	7.43 (1H, brs)	7.47 (1H, d, 2.0)	7.03 (1H, d, 7.4)	6.66 (1H, d, 7.6)
3	6.46 (1H, t, 8.0)	—	—	—	—	6.50 (1H, m)	6.49 (1H, t, 7.6)
4	6.30 (1H, d, 8.0)	6.58 (1H, brs)	6.59 (1H, d, 2.0)	6.66 (1H, brs)	6.69 (1H, d, 2.0)	6.50 (1H, d, 7.4)	6.36 (1H, d, 7.6)
5							
6							
7	6.56 (1H, d, 8.0)	6.69 (1H, d, 7.6)	6.69 (1H, dd, 8.0, 1.6)	6.73 (1H, d, 7.6)	6.75 (1H, dd, 8.0, 1.6)		
8	6.48 (1H, t, 8.0)	6.58 (1H, m)	6.57 (1H, t, 8.0)	6.58 (1H, m)	6.58 (1H, t, 8.0)	6.73 (1H, d, 8.0)	6.82 (1H,d, 7.6)
9	6.30 (1H, d, 8.0)	6.50 (1H, m)	6.46 (1H, dd, 8.0, 1.6)	6.60 (1H, m)	6.53 (1H, dd, 8.0, 1.6)	6.61 (1H, d, 8.0)	6.39 (1H,d, 7.6)
10	9.89 (1H, s)	10.31 (1H, brs)	Exchanged	9.76 (1H, brs)	Exchanged	10.05 (1H, brs)	9.68 (1H, s)
11							
12	A 7.69 (1H, brs) B7.28 (1H, brs)	A 7.78 (1H, brs) B 7.43 (1H, brs)	Exchanged	14.71 (1H, brs)	Exchanged	A 7.92 (1H, brs) B 7.36 (1H, brs)	Exchanged
13							
14	A 7.85 (1H, brs) B 7.28 (1H, brs)						
15	2.88 (3H, s)	7.68 (1H, m)	7.68 (1H, d, 7.5)	7.63 (1H, m)	7.62 (1H, d, 7.5)		
16		7.54 (1H, m)	7.51 (1H, t, 7.5)	7.54 (1H, m)	7.50 (1H, t, 7.5)		
17		7.63 (1H, m)	7.60 (1H, t, 7.5)	7.61 (1H, m)	7.57 (1H, t, 7.5)	7.32 (1H, m)	7.44 (1H, m)
18		7.54 (1H, m)	7.51 (1H, t, 7.5)	7.54 (1H, m)	7.50 (1H, t, 7.5)	7.36 (1H, m)	7.33 (1H, m)
19		7.68 (1H, m)	7.68 (1H, d, 7.5)	7.63 (1H, m)	7.62 (1H, d, 7.5)	7.36 (1H, m)	7.33 (1H, m)
20						7.36 (1H, m)	7.33 (1H, m)
21		A 8.08 (1H, brs) B 7.43 (1H, brs)	Exchanged	A 7.84 (1H, brs) B 7.46 (1H, brs)	Exchanged	7.32 (1H, m)	7.44 (1H, m)
22		2.95 (3H, s)	2.95 (3H, s)	2.98 (3H, s)	2.99 (3H, s)		
23						3.69 (3H, s)	3.76 (3H, s)
24						3.15 (3H, s)	3.27 (3H, s)

[a] DMSO-d_6. [b] DMSO-d_6 : CD_3OD 3 : 1. [c] $CDCl_3$.

Table 2 ^{13}C NMR data of dermacozines A–G (**1–7**)

No.	**1**[a] δ^{13}C/ppm, mult	**2**[a] δ^{13}C/ppm, mult	**3**[a] δ^{13}C/ppm, mult	**4**[b] δ^{13}C/ppm, mult	**5**[c] δ^{13}C/ppm, mult	**6**[a] δ^{13}C/ppm, mult	**7**[d] δ^{13}C/ppm, mult
1	112.3, C	111.2, C	107.4, C	110.9, C	131.7, C	131.9, C	131.8, C
2	121.2, CH	126.6, CH	129.2, CH	120.3, CH	127.1, CH	127.2, CH	127.3, CH
3	119.8, CH	128.4, C	127.9, C	120.2, CH	130.7, CH	130.9, CH	130.9, CH
4	116.0, CH	114.7, CH	114.3, CH	117.4, CH	119.6, CH	119.5, CH	119.7, CH
4a	138.8, C	138.9, C	138.8, C	138.7, C	133.7, C	133.8, C	133.6, C
5a	133.8, C	133.5, C	133.3, C	137.4, C	139.0, C	141.9, C	141.7, C
6	124.5, C	124.7, C	124.6, C	109.9, C	99.8, C	95.2, C	95.4, C
7	122.5, CH	123.9, CH	124.3, CH	140.3, C	139.6, C	142.7, C	142.5, C
8	121.6, CH	121.9, CH	121.6, CH	117.3, CH	133.8, CH	134.0, CH	133.7, CH
9	113.7, CH	114.8, CH	115.3, d	117.2, CH	130.2, CH	130.4, CH	129.9, CH
9a	138.0, C	135.8, C	134.5, C	138.6, C	150.2, C	150.4, C	150.3, C
10a	140.6, C	144.6, C	145.7, C	140.9, C	135.2, C	135.4, C	135.4, C
11	171.1, C	170.7, C	169.1, C	171.0, C	166.2, C	166.4, C	166.3, C
12							
13	171.2, C	194.1, C	193.6, C	166.6, C	164.5, C	162.5, C	—
14		138.4, C	138.3, C				
15	40.1, CH_3	129.9, CH	129.2, CH	86.6, C	161.8, C	160.5, C	—
16		129.1, CH	128.9, CH	137.2, C	121.7, C	119.7, C	119.8, C
17		132.6, CH	132.2, CH	126.6, CH	134.2, C	134.5, C	124.3, C
18		129.1, CH	128.9, CH	128.9, CH	131.2, CH	131.4, CH	132.3, CH
19		129.9, CH	129.2, CH	129.4, CH	128.1, CH	128.3, CH	115.2, CH
20		170.9, C	170.6, C	128.9, CH	127.7, CH	127.9, CH	158.3, C
21				126.6, CH	128.1, CH	128.3, CH	115.2, CH
22		40.0, CH_3	40.0, CH_3	169.6, C	131.2, CH	131.4, CH	132.3, CH
23				53.5, CH_3	45.9, CH_3	46.0, CH_3	46.3, CH_3
24				43.5, CH_3			

[a] At 100 MHz in DMSO-d_6. [b] At 100 MHz in $CDCl_3$. [c] At 150 MHz in DMSO-d_6. [d] Resonances were obtained from 2D-NMR (^{1}H–^{13}C HSQC and HMBC) spectral interpretation. — not observed.

groups (1682, 1674, 1667 cm^{-1}) while the UV/Vis spectrum showed absorption maxima at 482 (sh), 419, 294, 242 and 204 nm.

It was obvious from ^{1}H and ^{13}C NMR spectra in combination with 2D ^{1}H–^{13}C HSQC NMR data of **2** (Tables 1 and 2) that **2** belonged to the same class of reduced phenazine as **1**. A COSY experiment, using a mixture of DMSO-d_6 and CD_3OD to overcome the overlap of aromatic with exchangeable protons (ESI, Fig. S15 and S16†), allowed the construction of three spin systems (Fig. 1b): H-2, H-4, δ_H 7.43 (d, 2.0), δ_H 6.59 (d, 2.0); H-7, H-8, H-9, δ_H 6.69 (dd, 8.0, 1.6), 6.57 (t, 8.0), 6.46 (dd, 8.0, 1.6); and phenyl protons H-15/H-19, δ_H 7.68 (d, 7.5), H-16/H-18, δ_H 7.51 (d, 7.5) and H-17 δ_H 7.60 (t, 7.5). In addition the ^{13}C NMR spectrum revealed eight quaternary carbon atoms comprising three carbonyls: two amides C-11 (δ_C 170.7), C-20 (δ_C 170.9) and a ketone (C-13, δ_C 194.1 s), four nitrogenated carbons C-4a, C-5a, C-9a and C-10a (δ_C 138.9, 133.5, 135.8 and 144.6), and two olefinic carbons C-1 and C-6 (δ_C 111.2 and 124.7). Five hydrogen resonances lacked correlations in the ^{1}H–^{13}C HSQC NMR spectrum (DMSO-d_6) of **2** and were therefore recognized as being bonded to nitrogen and assigned as NH_2-12, δ_H 7.78, 7.43; NH_2-21, δ_H 8.08, 7.43 and NH-10 δ_H 10.31.

With all protons assigned to their directly attached carbon and nitrogen atoms, it was possible to deduce six substructures, and the connectivities between these substructures were established from key HMBC correlations (ESI, Table S1†). Thus, correlations from H-2 to C-11, and from H-2 and H-4 to C-10a, as well as from H-7 to C-20 and from H-8 to C-6, clearly defined the positions of the two amide groups. Moreover, correlations from the methyl group CH_3-15 to C-4a and C-5a confirmed its position relative to C-4a and C-5a. The position of the benzoyl moiety on C-3 was defined from HMBC correlations from H-2, H-4 and H-15/H-19 to C-13. Also, HMBC correlations from NH-10 to C-4a and C-5a confirmed the reduced phenazine skeleton.

Dermacozine C (**3**) was obtained as a reddish-brown substance. From high-resolution mass spectrometry the molecular formula was determined as $C_{22}H_{17}N_3O_4$, thus implying 16 degrees of unsaturation. The close similarity of the UV, IR and NMR data readily revealed **3** to be a derivative of **2** with a carboxylic acid group at C-11 [(δ_C 169.1) and OH-12 (δ_H 14.71, brs)] rather than the carboxamide group in **2** as evident from the one mass unit difference and the upfield shift of C-1 to δ_C 107.4 and a concomitant downfield shift of C-2 to δ_C 129.2 compared to δ_C 111.2 and δ_C 126.6 in **2**, respectively.[16] Key HMBC correlations from C-11 to H-2 as well as C-13 to H-2 and H-4 confirmed the positions of carboxylic acid and benzoyl groups at C-1 and C-3, respectively (ESI, Table S1†).

Dermacozine D (**4**) was obtained as an optically active golden yellow substance ($[\alpha]_D^{25} = +18$ (*c* 0.1, MeOH)). The molecular formula was established by accurate mass measurements as $C_{24}H_{19}N_3O_5$, which required 17 degrees of unsaturation. The IR absorption peaks of **4** suggested NH_2 (3348, 3322 cm^{-1}) and carbonyl groups (1751, 1723, 1672 cm^{-1}) while the UV/Vis spectrum showed absorption maxima at 452 (sh), 408, 264, 249 and 205 nm.

Comprehensive analysis of 1D and 2D-NMR data indicated a reduced phenazine backbone similar to **1**. The ^{1}H NMR spectrum ($CDCl_3$) of **4** indicated the presence of two methyl groups CH_3-23 (δ_H 3.76) and CH_3-24 (δ_H 3.27); while the ten aromatic methines discernible could be grouped by the COSY experiment (Fig. 1c) into three spin systems comprising H-2, H-3, H-4 [δ_H 6.66 (d, 7.6), 6.49 (t, 7.6), 6.36 d, 7.6)], H-8, H-9 [δ_H 6.82 (d, 7.6), 6.39 (d, 7.6)] and a monosubstituted benzene ring H-17 - H-21 [δ_H 7.44 (2H, m), 7.33 (3H, m)]. From the ^{13}C NMR spectrum, additionally twelve quaternary carbon atoms including three carbonyls C-11, C-13 and C-22 (δ_C 171.0, 166.6 and 169.6), nitrogenated carbons C-4a, C-5a, C-9a and C-10a (δ_C 138.7, 137.4, 138.6 and 140.9), and olefinic carbons C-1, C-6, C-7, C-15 and C-16 (δ_C 110.9, 109.9, 140.3, 86.1 and 137.2) were evident. Two exchangeable protons were observed in DMSO-d_6 attributed to NH_2-12 (δ_H 7.92, 7.36). Key HMBC correlations of **4** included H-2 to C-11, H-3 to C-1, H-2 and H-4 to C-10a, H-3 to C-4a, NH-10 and CH_3-24 to C-4a and C-5a, H-8 to C-9a and C-6 and H-9 to C-7. Finally, a correlation was also observed from CH_3-23 to C-22 as well as from H-8, and H-17/H-21 to C-15 to define the position of the phenyl moiety at C-15. The ^{13}C NMR chemical shift of C-15 was consistent with compounds having a similar five membered lactone ring.[17]

The absolute configuration at C-15 was determined as *S* by a combination of CD spectroscopy and time-dependent DFT-LDA calculations rather than using destructive derivatisation techniques which might have inverted the chiral centre at C-15. All calculations were performed with the ORCA electronic structure package version 2.6.71.[18] The compound was expected to contain a deprotonated ring nitrogen at neutral pH based on the low pK_a values of other phenazine derivatives, and for this reason both the neutral and anionic forms of **4** were used as input for the calculations. Both the *R* and *S* enantiomers of **4** were optimized at the DFT level using the PBE functional[19] and the SV basis set[20] with polarization functions on non-hydrogens.[21] The resolution of the identity approximation was employed in all calculations and used the SV/J auxiliary basis set.[22,23] Default settings were used for integration grids and convergence criteria. Solvent (ethanol) effects were incorporated in the geometry optimizations and the subsequent CD calculations using the COSMO model.[24]

TDDFT calculations of the CD spectra were performed within the local density approximation (LDA) using the SVWN functional.[25] Several basis sets were tried for the TDDFT calculations (data not shown), but overall the best results were obtained with Dunning's correlation consistent double ζ basis set (cc-pVDZ) which was used for final calculations.[26] The spectral lineshape (Fig. 2) was obtained by a Gaussian peak fitting to the calculated excitations. Based on the good agreement between the calculated anionic CD spectra and the experimental spectrum, a shift of –60 nm was applied to the calculated spectra in order to obtain a better overlay of peaks B and C (these being chosen as they were the sharpest and best defined peaks in the experimental spectrum). The complete difference in the calculated neutral (Fig. 2a (ii)) and anionic (Fig. 2a (i)) spectra along with the very good match of the anionic spectra to experiment suggests that the deprotonated form contributed most to the spectrum obtained experimentally. For this reason the anionic spectra were taken as unequivocal evidence that the absolute stereochemistry of the natural product was *S* (Fig. 2a (i)).

In order to investigate whether hydrogen-bonding of the amide side chain was particularly important in controlling the CD spectrum of dermacozine E in its deprotonated state, the conformational preference of this group in the *S*-form of the molecule was investigated by performing two optimizations at

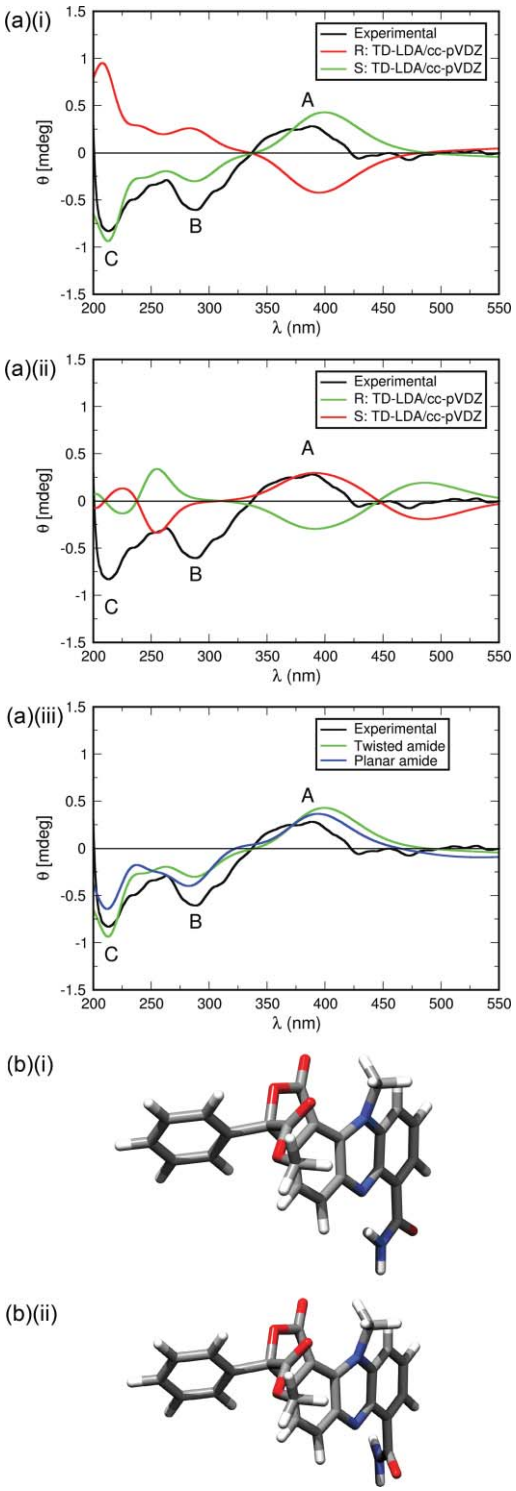

Fig. 2 (a) (i) Experimental CD spectrum for dermacozine D **4** compared with the calculated TD-LDA/cc-pVDZ CD spectra of its *S* and *R* enantiomers (deprotonated). (ii) Experimental CD spectrum for dermacozine D **4** compared with the calculated TD-LDA/cc-pVDZ CD spectra of its *S* and *R* enantiomers (protonated). (iii) Experimental CD spectrum for dermacozine D **4** compared with the calculated TD-LDA/cc-pVDZ CD spectra of its *S* enantiomer with twisted and planar amide rotamers. (b) (i) Optimized PBE/SV(P) geometry of the dermacozine D *S*-enantiomer **4** with planar amide group. (ii) Optimized PBE/SV(P) geometry of the dermacozine D *S*-enantiomer **4** with twisted amide group.

the PBE/SV(P) level in COSMO ethanol. The first of these had the amide group hydrogen bonded *via* its amido hydrogen to the deprotonated pyrazine ring nitrogen atom and the second was started with the amide group arranged perpendicular to the plane of the adjacent aromatic ring. These optimizations located two different minima, one planar and hydrogen bonded and the other at a dihedral angle of 48.8 degrees, measured from the amide oxygen to the ring carbon adjacent to the deprotonated nitrogen (Fig. 2b.) (i) and (ii), respectively. Single point calculations on these structures at the PBE/aug-cc-pVTZ level showed that the twisted form was 39.8 kJ mol^{-1} higher in energy than the planar system suggesting that the planar form would be dominant and that the twisted form should be of negligible importance.

Despite these energy differences, both rotamers were subsequently submitted for calculation of their CD spectra at the TD-LDA/cc-pVTZ level incorporating solvent (ethanol) effects approximately through the use of the COSMO method. The results of these calculations are shown in Fig. 2a (iii). Small changes are seen between the two structures suggesting that the rotation of the amide group has only a minimal effect on the CD spectrum. Interestingly, the best fit to the experimental spectrum appears to come from the high energy twisted amide rotamer which the DFT calculations indicated should not be significantly populated. This may be due to explicit solvent interactions in the experimental system which are missing in the continuum solvent model used in the calculations. Hydrogen bonding of ethanol alcohol hydrogen to the deprotonated ring nitrogen in dermacozine E would most probably occur in solution and (along with other specific solvent interactions) this might lower the relative energy of the twisted form, thus making its contribution to the CD spectrum more important. Despite the small rotameric effects in the calculated CD spectra, the conclusion that the *S* form is responsible for producing the experimental spectrum remains unchanged.

Dermacozine E (**5**) was obtained as a bluish violet substance. The molecular formula was determined as $C_{23}H_{16}N_4O_3$ from HRESIMS, which required 17 degrees of unsaturation. The IR absorption suggested NH_2 (3347, 3324 cm^{-1}) and carbonyl groups (1736, 1710, 1682 cm^{-1}). The UV/Vis spectrum of **5** showed absorption maxima at 621 (sh), 576, 534 sh, 363, 270 nm, which displayed significant hyperchromic and bathochromic shifts upon addition of NaOH but no noticeable effect upon addition of HCl (ESI, Figure S39A†).

The ^1H and ^{13}C NMR spectra of **5** (Tables 2 and 3) exhibited one methyl signal at δ_H 3.68 (CH_3-23), ten aromatic methine groups comprising three spin systems as described above for dermacozine D (**4**) and additionally eleven quaternary carbon atoms including three carbonyls C-11, C-13 and C-15 (δ_C 166.2, 164.5 and 161.8), nitrogenated carbons C-4a, C-5a, C-9a and C-10a (δ_C 133.7, 139.0, 150.2 and 135.2), and olefinic carbons C-6, C-16, C-1, C-17 and C-7 (δ_C 99.8, 121.7, 131.7, 134.2 and 139.6), respectively.

Protons were assigned to their directly bonded carbons by a ^1H–^{13}C HSQC NMR spectrum, but three hydrogen resonances lacked correlations to carbons and were therefore recognized as being located on either oxygen or nitrogen. Connectivities between the three spin systems were established from key ^1H–^{13}C HMBC correlations (ESI, Table S1†). Thus, correlations from H-3 and H_2-12 to C-1 and from H-2 to C-11 clearly defined the position of the amide group on C-1. Moreover, correlations from H-2 and H-4 to C-10a, as well as from H-3 to C-4a, defined the positions of

Table 3 ^{1}H NMR data of dermacozines E–G (**5–7**)

No.	**5**[a] δ^1H/ppm, mult, J/Hz	**6**[b] δ^1H/ppm, mult, J/Hz	**7**[b] δ^1H/ppm, mult, J/Hz
1			
2	8.02 (1H, d, 8.0)	8.01 (1H, d, 8.0)	8.00 (1H, d, 8.0)
3	7.78 (1H, t, 8.0)	7.76 (1H, t, 8.0)	7.77 (1H, t, 8.0)
4	7.95 (1H, d, 8.0)	7.94 (1H, d, 8.0)	7.96 (1H, d, 8.0)
5			
6			
7			
8	7.20 (1H, d, 9.6)	7.17 (1H, d, 9.5)	7.21 (1H, d, 9.6)
9	7.30 (1H, d, 9.6)	7.28 (1H, d, 9.5)	7.35 (1H, d, 9.6)
10			
11			
12	A. 8.84 (1H, brs) B. 7.86 (1H, brs)	A. 8.83 (1H, brs) B. 7.86 (1H, brs)	A. 8.71 (1H, brs) B. 7.84 (1H, brs)
13			
14	11.26 (1H, brs)		
15			
16			
17			
18	7.31 (1H, d, 8.0)	7.29 (1H, d, 8.0)	7.11 (1H, d, 8.0)
19	7.48 (1H, t, 8.0)	7.46 (1H, t, 8.0)	6.82 (1H, d, 8.0)
20	7.42 (1H, t, 8.0)	7.39 (1H, t, 8.0)	(OH) 7.18 (1H, brs)
21	7.48 (1H, t, 8.0)	7.46 (1H, t, 8.0)	6.82 (1H, d, 8.0)
22	7.31 (1H, d, 8.0)	7.29 (1H, d, 8.0)	7.11 (1H, d, 8.0)
23	3.68 (3H, s)	3.68 (3H, s)	3.66 (3H, s)

[a] At 400 MHz in DMSO-d_6. [b] At 600 MHz in DMSO-d_6.

C-10a and C-4a relative to the position of olefinic spin system H-2, H-3 and H-4. HMBC correlations from H-9 to C-5a and from H-8 to C-9a and C-6 confirmed the positions of C-6, C-9a and C-5a relative to the olefinic spin system H-8, H-9. The position of the methyl group CH_3-23 can be easily defined through its HMBC correlations to C-4a and C-5a with an additional long range correlation (^4J) to C-4 (Fig. 1d). Finally, the HMBC spectrum showed clear correlations from H-8, H-18, H-22 to C-16 with a long range correlation (^4J) from H-9 to C-16 to confirm the position of monosubstituted benzene ring. Additional long-range correlations were obtained from a long range ^{1}H–^{13}C HMBC (J = 3 Hz) of H-4 to C-1 (^4J), of H-2 to C-4a (^4J), of H-3 to C-10a (^4J) and C-11 (^4J), of H-8 to C-5a (^4J) and C-15 (^4J) and finally H-9 to C-13 (^5J) to confirm the C-13 and C-15 positions (Fig. 1d). The observed $^4J/^5J$ were consistent with known coupling constants for such systems ($^4J \approx 1.11$ Hz) and ($^5J \approx 0.48$ Hz) (Fig. 1d).[27]

From the results of a ^{1}H–^{15}N HSQC experiment it was evident that three protons were bonded to nitrogen; comprising of one NH_2 group; NH_2-12 (δ_H 8.84, 7.86) and NH-14 (δ_H 11.26). From the ^{1}H–^{15}N HMBC NMR spectrum of **5** it was possible to assign the resonance of each nitrogen: NH_2-12 (δ_N 113.2) NH-14 (δ_N 170.2), N-5 (δ_N 136.1) and N-10 (δ_N 301.1) (Fig. 1e). The position of N-14 in a carboxylic imide moiety was confirmed by ^{1}H–^{15}N HSQC and ^{1}H–^{13}C HMBC that showed a correlation from a strong downfield shifted H-14 (δ_H 11.26, brs) to N-14 (δ_N 170.2) as well as to C-6, C-16 which defined its position between two carbonyl groups, and was also compatible with the reported shifts in previously isolated compounds that have the same system.[28,29] Also, it was possible to define the positions of other nitrogens using ^{1}H–^{15}N HMBC data that showed correlations from H-4 and H-23 to N-5 (δ_N 136.1) and from H-9 to N-9 (δ_N 301.1) (Fig. 1e). A comparison of the UV spectrum of **5** with that obtained *via* TDDFT calculations confirmed the structure proposed.

Two geometry optimizations with subsequent calculations of absorption spectra were performed. In all calculations on Dermacozine E the ethanol solvent environment was simulated using the COSMO dielectric continuum solvation model. The first approach used the generalized gradient approximation (GGA) with the PBE exchange–correlation functional in combination with the triple-ζ TZVP basis set of Ahlrichs *et al.*[20,23] for the optimization stage. This geometry was then used in a TD-PBE/TZVP++ (the same basis set augmented with diffuse functions on all atoms) TDDFT calculation of the absorption spectrum. The first 25 excitations were included.

The second approach chosen employed the more recently developed *meta*-GGA approximation which makes use of a more complicated functional of the charge density involving the gradient of the kinetic energy density. The same procedure was followed as for the GGA calculations but the TPSS *meta*-GGA functional was substituted for the PBE functional used previously.

In both cases the final geometry of the dermacozine E (**5**) structure was found to have a strained appearance due to the presence of the N-methyl group interacting with the nearby carbonyl oxygen attached to C-12. Fig. 3a and 3b show the PBE/TZVP geometry (for viewing purposes identical to the TPSS/TZVP geometry) in stick and space-filling representations. The distortion is most clearly shown in stick Fig. 3a whilst the steric crowding can be seen in the space-filling representation in Fig. 3b.

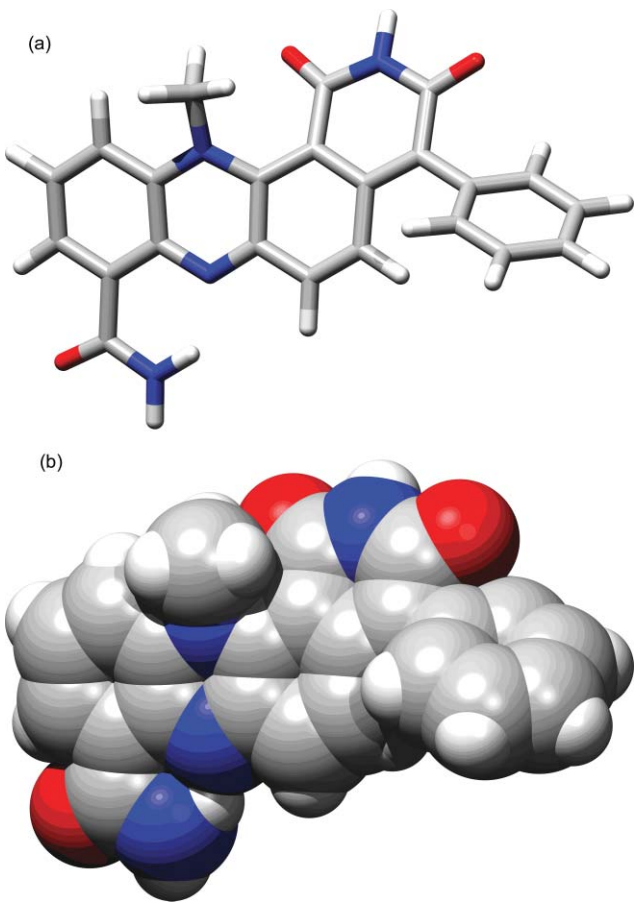

Fig. 3 Optimized PBE/TZVP geometry of dermacozine E (**5**).

The TD-PBE/TZVP++ and TD-TPSS/TZVP++ spectra are shown in Fig. 4. The two calculated spectra are essentially identical in general form and position of the peaks. The most noticeable difference is the blue-shift of the TD-TPSS spectrum relative to that obtained with the PBE functional. This effect may be due to an improved exchange–correlation potential arising from the use of the *meta*-GGA functional as more conventional pure exchange–correlation functionals such as PBE commonly underestimate excitation energies. The TD-PBE (TD-TPSS) peaks appear at approximately 325 (310), 400 (390) and 540 (525) nm which is consistent with the observed UV spectrum (Fig. 4).

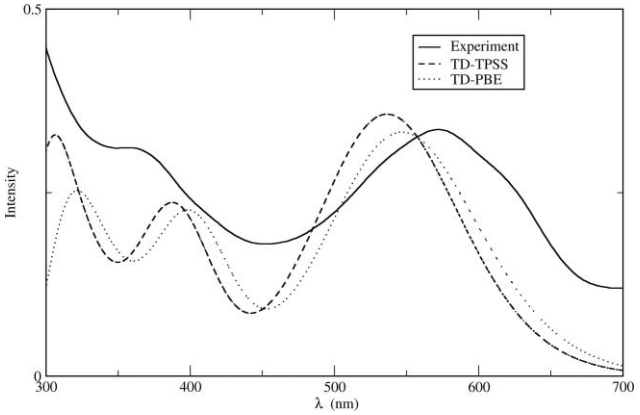

Fig. 4 Experimental and calculated absorption spectra for dermacozine E (**5**).

Dermacozine F (**6**) was obtained as a bluish violet substance. The molecular formula was determined as $C_{23}H_{15}N_3O_4$ by HRESIMS spectrometry, which required 17 degrees of unsaturation. This suggested the exchange of one NH in **5** by an oxygen atom in **6**. This was corroborated by the ^{1}H NMR spectrum of **6** which indeed lacked a NH-14 signal which was thus substituted for an oxygen atom to form a carboxylic anhydride moiety in **6** instead of imide in **5**. Correspondingly the ^{13}C NMR showed upfield shifts for C-13, C-15 and C6 (δ_C 162.5, 160.5 and 95.2) in comparison to the respective signals in **5** (δ_C 164.5, 161.8 and 99.8).[16]

Dermacozine G (**7**) was isolated as a minor compound and obtained as a bluish violet substance. The molecular formula was determined as $C_{23}H_{15}N_3O_5$ by HRESIMS corresponding to one additional oxygen atom in comparison to **6**. The ^{1}H and ^{13}C NMR data readily established that **7** was the 20-hydroxy congener of **6** as evident from the characteristic AA′XX′ spin system in the ^{1}H NMR spectrum and the downfield chemical shift for C-20 (δ_C 158.3).

Hypothetical biogenetic pathway

The strains were previously screened to assess their biosynthetic potential, using sets of degenerate primers to detect the presence of NRPS, PKS type I and II sequences in the corresponding genomes. Non-ribosomal peptide synthetase sequences were detected only in strain MT1.2, whereas neither PKS–I or II were detected in strain MT1.1 or MT1.2.[6]

Dermacozines like most phenazine natural products are believed to be derived *via* the shikimic acid pathway, as outlined in Scheme 1, with chorismic acid as the most probable branch point intermediate. Shikimic acid is converted to chorismic acid in known transformations that are part of the aromatic amino acid biosynthetic pathway.[14,30–32] The transformation from chorismic acid to the phenazine precursors is catalyzed by a series of phenazine synthesis-specific enzyme-controlled steps to give *trans*-2,3-dihydro-3-hydroxyanthranilic acid (DHHA).[33–35] Two molecules of DHHA can self condense to form phenazine-1,6-dicarboxylic acid (**9**).[33,36–40] An alternative pathway would proceed *via* aminodehydroquinic acid to 5-amino-5-deoxyshikimic acid, which upon dehydration, self condensation, and oxidation could lead to the formation of phenazine-1,6-dicarboxylic acid (**9**) or its reduced form (e.g **1**), which are the main precursors for more complex phenazine metabolites.[38,41]

Phenazine-1,6-dicarboxylic acid would at some stage undergo *N*-methylation and single or double amide bond formation yielding a dermacozine A-type biogenetic intermediate.[42] This would couple to a C_6–C_1 or C_6–C_2 building block to yield dermacozine B/C compounds or dermacozine D–G congeners. In this context it is interesting to note that both phenylacetic acid and its amide were detected in the culture medium.

As previously discussed, the dermacozines are phenazine alkaloids, and in nature the phenazines are formed by cells that have stopped dividing and metabolise slowly. Phenazine metabolites have no obvious function for cell growth, *i.e.* no importance as energy sources or reserve substances of any kind. The lack of obvious metabolic functions of phenazines has led to several hypotheses on their physiological role in nature. It has been shown that phenazine-producing organisms survive longer in their natural environment compared to non-phenazine-producing species.[14] Therefore, it is likely that the phenazines represent a bacterial defence factor, due to their apparent antibiotic activity, which serves to protect the producing organism and its habitat against other microorganisms and microbial competitors, and thus improves the living conditions for the host organism.[14]

Other known biological activities are antioxidant, antitumour, antimalarial and antiparasitic. The possible mode of action is the inhibition/control of DNA (intercalation or groove binding), RNA and protein synthesis as well as disruption of energy requiring membrane-associated metabolic processes.[14]

Biological activity data

During the last decade, various bioactivities of phenazines have been characterised. The anti-bacterial activity of this class[43,44] is associated to its capacity to generate free radicals.[45] However, substituted phenazines have been reported to exhibit radical scavenging properties due to the presence of aromatic or unsaturated isoprenyl functional chains, and for this reason antioxidant activity was measured.[14,46,47] Recently, antitumour activity of a variety of phenazines has been reported on various cancer cell lines.[48–51] Due to these prior results, we evaluated the antitumour activity of the isolated phenazines on the resistant cancer cell line K562 (human chronic myelogenous leukemia).

In agreement with earlier reports for phenazines of different sub-classes,[48–51] dermacozines A–G (**1–7**) showed cytotoxic activity against this resistant cancer cell line at a low μM range. The highest cytotoxic potency was observed for dermacozines F (**6**) and G (**7**) with IC_{50} values of 9 and 7 μM, respectively (Table 4).

Radical scavenging activity and antioxidative potential of **1–7** against stable DPPH$^\bullet$ was determined spectrophotometically. A

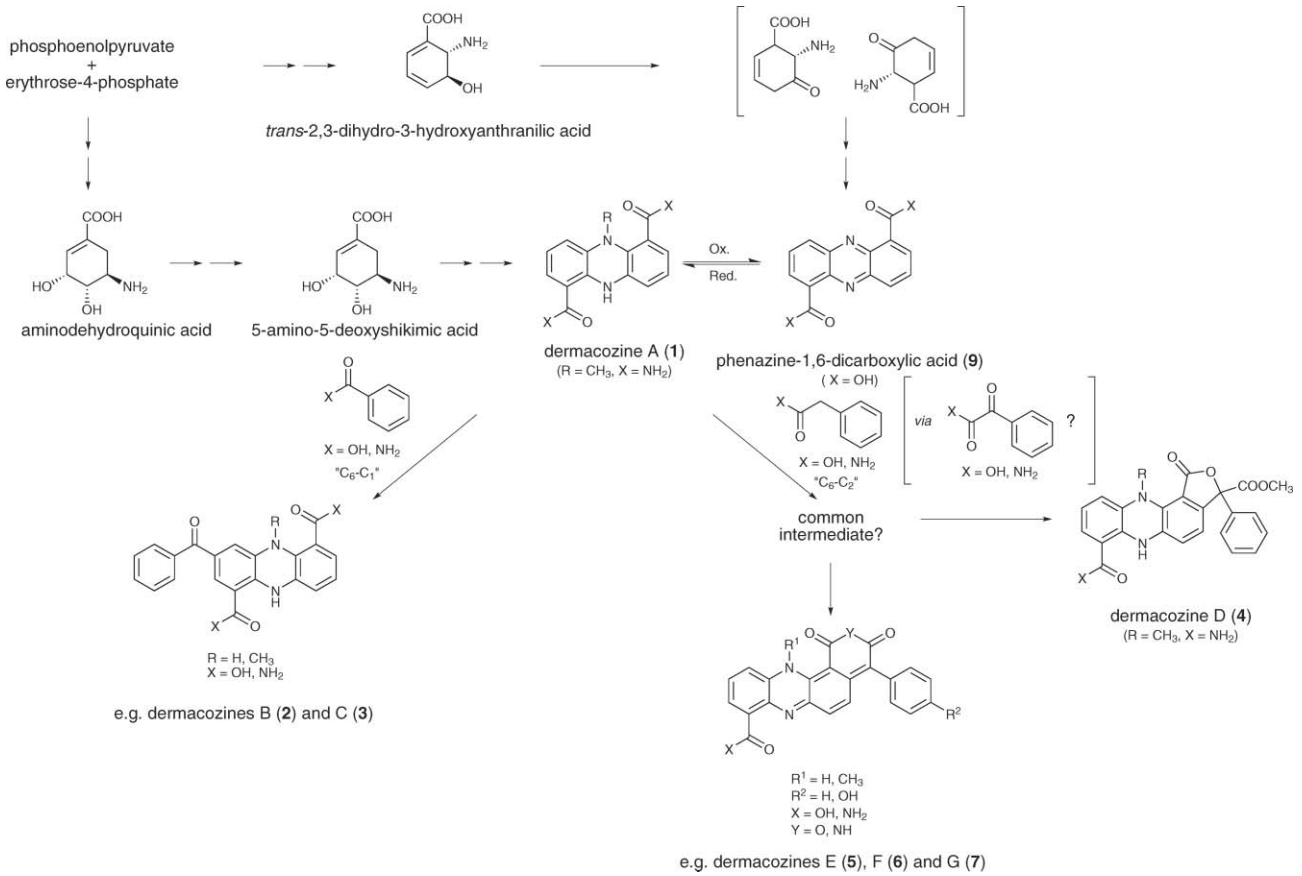

Scheme 1 Proposed biogenetic scheme for the dermacozines.

Table 4 Biological activity of the dermacozines

Compound	K562 Cytotoxicity $IC_{50}/\mu M$	DPPH radical scavenging activity $IC_{50}/\mu M$
Dermacozine A	140	77.5
Dermacozine B	220	38.0
Dermacozine C	180	8.4
Dermacozine D	100	106.9
Dermacozine E	145	—
Dermacozine F	9	—
Dermacozine G	7	—
Ascorbic acid		12.1

rapid TLC screening method exhibited four active compounds (**1**, **2**, **3**, **4**) appearing as yellow spots against purple background.[52,53] A confirmatory spectrophotometric assay was carried out for these according to a previously reported method,[54] using ascorbic acid as a positive control. The percentage reduction of the DPPH profile was measured at 517 nm and the IC_{50} was calculated and shown in Table 4.[55–58]

Dermacozine C (**3**) displayed the strongest radical scavenging activity (IC_{50} 8.4 μM) followed by dermacozine B (**2**) (IC_{50} 38.0 μM) while dermacozines A (**1**) and D (**4**) had the weakest antioxidant activity (IC_{50} 77.5 and 106.9 μM, respectively). Only dermacozine C (**3**) was more potent than ascorbic acid (IC_{50} 12.1 μM). Obviously a fully reduced skeleton is required for antioxidant activity of the dermacozines while oxidation as in **5-7** abolishes it. Carboxamide groups at C-1 and C-6 potentiate the activity as in **1** and removal or replacing of any of them by a cyclic ester as in **4** leads to a decrease in the activity. Replacement of carboxamide by carboxylic acid groups increases the activity. Furthermore, substitution at C-3 by a benzoyl group as in **2** and **3** has a positive effect.

Conclusion

The dermacozines are a novel class of phenazine isolated from the fermentation of deep-sea piezotolerant *Dermacoccus abyssi*, MT1.1 and MT1.2, recovered from the Mariana Trench sediment at depth of 10 898 m, using ISP2 and a complex medium 410, respectively. Cytotoxic activity on the K562 cell line as well as radical scavenging activity of these compounds were assessed. Dermacozines F (**6**) and G (**7**) exhibited moderate cytotoxic activity against leukaemia cell line (K562) with IC_{50} values of 9 and 7 μM, respectively, while the highest radical scavenger activity was observed with dermacozine C (**3**) with an IC_{50} value of 8.4 μM. We are currently culturing *Dermacoccus abyssi* at pressures of up to 60 MPa (6000 m depth equivalent), which will yield environmentally relevant information about the physiology of this organism as well as provide information on how its secondary metabolite complement varies with pressure.

Experimental section

General experimental procedures

^{1}H, ^{13}C and all NMR 2D experiments were recorded on Varian Unity INOVA 600 equipped with a cryoprobe and Varian Unity INOVA 400 MHz NMR systems. Low resolution ESI-MS data were obtained using a Perseptive Biosystems Mariner LC-MS, and high-resolution ESI-MS data were obtained on a Finnigan MAT 900 XLT system. HPLC separations were carried out using a Phenomenex reversed-phase column (Jupiter 4 μm Proteo 90 Å, 250 × 10 mm, 4 μm) and an Agilent 1200 series gradient pump monitored using a DAD G1315B variable-wavelength UV detector.

Microorganisms

Dermacoccus abyssi strains MT1.1 and MT1.2 were isolated from Mariana Trench sediment (sample no. 281), collected at a depth of 10 898 m (Challenger Deep; 11°19′911″ N; 142°12′372″ E) by the remotely operated submarine *Kaiko*, using a sterilized mud sampler, on 21/05/1998, during dive number 74.[6] No special precautions were made to maintain the sediment at high pressure. The sample was transported to the UK in an insulated container at 4 °C and stored at –20 °C until analysed for actinomycetes. Strains were purified and supplied by the School of Biology, University of Newcastle, UK.

Fermentation conditions

For *Dermacoccus abyssi* strain MT 1.1, the first-stage seed was performed by inoculation of an agar grown culture into 10 mL of GYE medium (4.0 g glucose, 4.0 g yeast extract, distilled water 1 L adjusted to pH 7.0). After 5 days incubation at 28 °C with agitation at 150 rpm, the first stage was used to inoculate the production fermentation, using ISP2 medium (4.0 g yeast extract, 10 g malt extract, 4.0 g glucose, 2 g $CaCO_3$, distilled water 1 L adjusted to pH 7.3) in the presence of HP20 resin at 28 °C with agitation at 150 rpm and then harvested after 7 days. Cultivation of strain MT 1.2 was carried out in 500 mL Erlenmeyer flasks with one baffle containing 100 mL of complex medium 410 (glucose 10 g, glycerol 10 g, oatmeal 5 g, soybean meal 10 g, yeast extract 5 g, Bacto casamino acids 5 g and $CaCO_3$ 1 g in 1 L tap water, adjusted to pH 7.0). Shake flasks were inoculated with 4% by volume of a shake-flask pre-culture grown in the same medium for 72 h, and were incubated on a rotary shaker at 120 rpm and 27 °C for 144 h.

Compound isolation and purification procedures

Harvested fermentation broth from strain MT 1.1 (15 L) was centrifuged at 3000 rpm for 20 min, and the HP20 resin together with the cell mass was washed with distilled water and then extracted with methanol (5 × 500 mL). The successive MeOH extracts were combined and concentrated under reduced pressure yielding 250 mL of materials that were extracted with n-hexane (3 × 250 mL) and EtOAc (5 × 250 mL). The EtOAc fraction was subjected to purification by Sephadex LH-20 column chromatography (CH_2Cl_2–MeOH 1 : 1) to give three fractions. Final purification was achieved by reversed–phase HPLC (Jupiter 4 μm Proteo 90 Å, 250 × 10 mm, 4 μm) using a gradient of 0–90% CH_3CN–H_2O over 40 min. Fraction A (121 mg) afforded dermacozine A (**1**) (49.5 mg); fraction B (37 mg) afforded dermacozine B (**2**) (12.9 mg) and D (**4**) (17.4 mg); and fraction C (106 mg) afforded dermacozine E (**5**) (31.2 mg), F (**6**) (8.5 mg) and G (**7**) (1.6 mg) respectively.

The culture broth from strain MT 1.2 was separated by centrifugation into supernatant and biomass, and the latter was discarded. The supernatant (8.5 L) was applied to an Amberlite XAD-16 column (resin volume 1 L) and the resin was washed with water. Dermacozines were eluted with H_2O–MeOH 4 : 6, concentrated *in vacuo* to an aqueous residue which was adjusted to pH 4 and extracted four times with EtOAc. The organic extracts were combined and concentrated *in vacuo* to dryness (409 mg). The crude product was dissolved in CH_2Cl_2 and added to a diol-modified silica gel column (45 × 2.6 cm; LiChroprep Diol, Merck). The separation was accomplished by a linear gradient from n-hexane–CH_2Cl_2 (1 : 1) to CH_2Cl_2–MeOH (9 : 1) within 4 h at a flow rate of 5 mL min^{-1}. Fractions containing discrete dermacozines were purified by Sephadex LH-20 and Toyopearl HW40-F (each column 90 × 2.5 cm) using MeOH–CH_2Cl_2 (2 : 1) as eluent.

HPLC-DAD analyses

The chromatographic system consisted of a HP 1090M liquid chromatograph equipped with a diode-array detector and a HP Kayak XM 600 ChemStation (Agilent). Multiple wavelength monitoring was performed at 210, 230, 260, 280, 310, 360, 435 and 500 nm, and UV/Vis spectra measured from 200 to 600 nm. A 10 mL aliquot of the fermentation broth was centrifuged, and the supernatant adjusted to pH 4 and extracted with the same volume of EtOAc. After centrifugation, the organic layer was concentrated to dryness *in vacuo* and re-suspended in 1 mL MeOH. 10 μL aliquots of the samples were injected onto an HPLC column (125 × 4.6 mm) fitted with a guard-column (20 × 4.6 mm) filled with 5 μm Nucleosil-100 C-18. The samples were analysed by linear gradient elution using 0.1% *ortho*-phosphoric acid as solvent A and CH_3CN as solvent B at a flow rate of 2 mL min^{-1}. The gradient was from 0% to 100% for solvent B in 15 min with a 2 min hold at 100% for solvent B.

Dermacozine A (1). Fluorescent yellowish green powder, 49.5 mg; UV: λ_{max}^{EtOH} (log ε) 398 (3.4), 270 sh (3.6), 254 (3.8), 208 (3.9) nm; IR (NaCl) ν_{max} 3359, 3328, 3010, 1681, 1673, 1591, 1534, 1467, 1415, 1322, 1248, 1175, 860, 778, 735, 710, 680 cm^{-1}; LRESIMS *m/z* 304.99 $[M+Na]^+$; HRESIMS (*m/z* 283.11866 $[M+H]^+$ calcd for $C_{15}H_{15}N_4O_2$, 283.11949, Δ = –2.9 ppm); ^{1}H and ^{13}C NMR data (DMSO-d_6), see Tables 1 and 2.

Dermacozine B (2). Reddish brown powder, 12.9 mg; UV: λ_{max}^{EtOH} (log ε) 482 sh (3.3), 419 (3.4), 294 (3.8), 242 (3.9), 204 (4.1) nm; IR (NaCl) ν_{max} 3344, 3214, 2963, 1682, 1674, 1667, 1561, 1533, 1487, 1265, 1321, 795, 740, 721 cm^{-1}; LRESIMS *m/z* 387.1 $[M + H]^+$, 409.0 $[M+Na]^+$; HRESIMS (*m/z* 387.14551 $[M+H]^+$ calcd for $C_{22}H_{19}N_4O_3$, 387.145713, Δ = –0.5 ppm); ^{1}H and ^{13}C NMR data (DMSO-d_6), see Tables 1 and 2.

Dermacozine C (3). Reddish brown powder, 13 mg; UV: λ_{max}^{EtOH} (log ε) 460 (4.0), 410 sh (3.9), 294 (4.3), 240 (4.5), 213 (4.5), 204 (6.5) nm; IR (NaCl) ν_{max} 3447, 3328, 3010, 2963, 1704, 1676, 1664, 1640, 1562, 1535, 1483, 1448, 1321,1265, 1228, 1184, 1050, 901, 873, 795, 740, 721 cm^{-1}; LRESIMS *m/z* 387.9 $[M+H]^+$ and 385.9 $[M - H]^-$; HRESIMS (*m/z* 387.12150 $[M]^+$ calcd for

$C_{22}H_{17}N_3O_4$, 387.12190, $\Delta = -1.0$ ppm); ^{1}H and ^{13}C NMR data (DMSO-d_6), see Tables 1 and 2.

Dermacozine D (4). Golden yellow powder, 17.4 mg; $[\alpha]_D^{25} = +18$ (c 0.1, MeOH); UV: λ_{max}^{EtOH} (log ε) 452 sh (3.6), 408 (3.7), 264 (4.2), 249 (4.2), 205 (4.4) nm; IR (NaCl) ν_{max} 3348, 3322, 2989, 1751, 1723, 1672, 1628, 1603, 1538, 1464, 1401, 1335, 1279, 1173, 1028, 928, 879, 761, 737, 710, 693 cm^{-1}; LRESIMS m/z 452.18 [M+Na]$^+$; HRESIMS (m/z 430.13974 [M+H]$^+$ calcd for $C_{24}H_{19}N_3O_5$, 430.14029, $\Delta = -1.3$ ppm); ^{1}H and ^{13}C NMR data (DMSO-d_6), see Tables 1 and 2.

Dermacozine E (5). Bluish violet amorphous powder, 31.2 mg; UV: λ_{max}^{EtOH} (log ε) 621 sh (3.8), 576 (3.9), 534 sh (3.8), 363 (3.8), 270 (4.2) nm, $\lambda_{max}^{EtOH+NaOH}$ (log ε) 625 sh (5.8), 583 (6.1), 543 sh (5.8), 364 (5.8) nm, $\lambda_{max}^{EtOH+HCl}$ 621 sh (3.9), 575.0 (4.0), 534 sh (3.9), 363 (3.9) nm; IR (NaCl) ν_{max} 3347, 3324, 1736,1710, 1682, 1631, 1610, 1549, 1469, 1402, 1345, 1263, 1177, 1125, 885, 763, 735, 695 cm^{-1}; LRESIMS m/z 419.20 [M+Na]$^+$; HRESIMS (m/z 397.12966 [M+H]$^+$ calcd for $C_{23}H_{17}N_4O_3$, 397.13006, $\Delta = -1.0$ ppm); ^{1}H and ^{13}C NMR data (DMSO-d_6), see Tables 2 and 3.

Dermacozine F (6). Bluish violet powder, 8.5 mg; UV: λ_{max}^{EtOH} (log ε) 621 sh (3.6) 566 (3.8), 372 (3.86), 263 (4.3), 251 (4.4) nm; IR (NaCl) ν_{max} 3339, 1783, 1735, 1677, 1648, 1596, 1544, 1513, 1448, 1407, 1258, 1181, 1030, 915, 845, 783, 727 cm^{-1}; LRESIMS m/z 398.1 [M+H]$^+$, 420.0 [M+Na]$^+$; HRESIMS (m/z 398.11299 [M+H]$^+$ calcd for $C_{23}H_{16}N_3O_4$, 398.114078, $\Delta = -2.7$ ppm); ^{1}H and ^{13}C NMR data (DMSO-d_6), see Tables 2 and 3.

Dermacozine G (7). Bluish violet powder, 1.6 mg; UV: λ_{max}^{EtOH} (log ε) 622 sh (3.7), 580 (3.9), 368 (3.6), 267 (4.1), 248 (4.5) nm; IR (NaCl) ν_{max} 3457, 3361, 3010,1778, 1744, 1679, 1644, 1600, 1535, 1509, 1443, 1322, 1229, 1198, 923, 866, 772, 719 cm^{-1}; LRESIMS m/z 412.0 [M − H]$^-$; HRESIMS (m/z 414.109091 [M+H]$^+$ calcd for $C_{23}H_{16}N_3O_5$, 414.108992, $\Delta = 0.2$ ppm); ^{1}H and ^{13}C NMR data (DMSO-d_6), see Tables 2 and 3.

Cytotoxic activity on K562 cells

1. Cell culture. K562 cells (human chronic myelogenous leukemia cells) were grown in RPMI 1640 medium (Bio-Whittaker) supplemented with 10% fetal bovine serum (FBS) and 1% antibiotic and antimycotic solution (AB) (Bio-Whittaker). Cells were maintained at 37 °C in a humidified atmosphere with 5% CO_2.

2. Cytotoxic activity on K562 cells. After 24 h of culture in 10% FBS and 1% AB medium, cells were centrifuged, re-dissolved in 0.1% FBS–1% AB medium at a concentration of 1×10^6 cells per mL and plated on a 24 multi-well plate. The purified testing compounds were added at concentration from 1 to 50 μg mL^{-1} to different wells. After an incubation time of 24 h at 37 °C in a humidified incubator at 5% CO_2, the cells were plated in 96 well plate (4 fractions of 75 μL per well). Cell viability was then evaluated following the manufacturer's protocol (CellTiter-Glo® Luminescent Cell Viability Assay, Promega). The luminescence was recorded with a Berthold Orion luminometer. The concentration that induced 50% inhibition of cell growth (IC_{50}) was evaluated.

DPPH radical-scavenging assay

Firstly, radical scavenging activity of dermacozines against stable DPPH·(2,2-diphenyl-2-picrylhydrazyl hydrate, Sigma-Aldrich) was performed with a rapid TLC screening method using 0.2% DPPH in MeOH. 30 min after spraying, the active compounds appeared as yellow spots against purple background.[52,53] Subsequently, a quantitative spectrophotometric assay was carried out.[47] Briefly, a 2.0 mL of a wide range of concentrations (2.5-120 μM) of test sample (in MeOH) was added to 2.0 mL of 100 μM of methanolic solution of DPPH. The mixture was vortexed for 1 min and then left to stand at room temperature for 30 min in dark. Absorption was measured at 517 nm on a UV-Vis spectrometer (Perkin-Elmer Instruments, Lambda 25). All experiments were carried out in triplicate, using ascorbic acid as a positive control. The percentage reduction Q of DPPH, Q, was calculated by the following formula:[47–51] Q (% Inhibition) $= [(A_B - A_A)/A_B] \times 100$ where: A_B-absorption of blank sample ($t = 0$ min); A_A-absorption of tested extract solution ($t = 30$ min).

Acknowledgements

The authors are grateful to EPSRC National Mass Spectrometric Centre, University of Wales, Swansea, for mass spectrometric analysis. We also thank Sharon M. Kelly, Institute of Biomedical and Life Sciences, University of Glasgow, for CD measurements. We thank the *Kaiko* operation team and the crew of M.S. *Yokosuka* for collecting sediment samples. WMAM thanks the Egyptian Government for a Ph.D. scholarship. ATB thanks the Leverhulme Trust for an Emeritus Fellowship. MJ is the recipient of a BBSRC Research Development Fellowship. This work also was supported in part by the "Recherche Cancer et Sang" foundation, Têlêvie and the "Recherches Scientifiques Luxembourg (RSL)" association. MS is supported by a Têlêvie grant. The authors thank the "Action Lions Vaincre le Cancer" and "Een Häerz fir kriibskrank Kanner" asbl for additional support. BFM thanks the Portuguese Foundation for Science and Technology for financial support (PTDC/FIS/73578/2006). All theoretical calculations were performed using the RINH/BioSS Beowulf cluster which is funded by the Scottish Government Rural and Environment Research and Analysis Directorate at the University of Aberdeen Rowett Institute of Nutrition and Health, Scotland with the assistance of Dr Tony Travis.

References

1 D. J. Newman and G. M. Cragg, *J. Nat. Prod.*, 2004, **67**, 1216–1238.
2 T. F. Molinski, D. S. Dalisay, S. L. Lievens and J. P. Saludes, *Nat. Rev. Drug Discovery*, 2009, **8**, 69–85.
3 T. Simmons, E. Andrianasolo, K. McPhail, P. Flatt and W. H. Gerwick, *Mol. Cancer Ther.*, 2005, **4**, 333–342.
4 A. T. Bull and J. E. Stach, *Trends Microbiol.*, 2007, **15**, 491–499.
5 H.-P. Fiedler, C. Bruntner, A. T. Bull, A. C. Ward, M. Goodfellow, O. Potterat, C. Puder and G. Mihm, *Antonie van Leeuwenhoek*, 2005, **87**, 37–42.
6 W. Pathom-Aree, J. E. Stach, A. C. Ward, K. Horikoshi, A. T. Bull and M. Goodfellow, *Extremophiles*, 2006, **10**, 181–189.
7 K. Taira, S. Kitagawa, T. Yamashiro and D. Yanagimoto, *J. Oceanogr.*, 2004, **60**, 919–926.
8 D. Skropeta, *Nat. Prod. Rep.*, 2008, **25**, 1131–1166.
9 W. Fenical and P. R. Jensen, *Nat. Chem. Biol.*, 2006, **2**, 666.
10 K. S. Lam, *Curr. Opin. Microbiol.*, 2006, **9**, 245.

11 E. B. Shirling and D. Gottlieb, *Int. J. Syst. Bacteriol.*, 1966, **16**, 313–340.
12 R. E. Gordon and J. M. Mihm, *Ann. N. Y. Acad. Sci.*, 1962, **98**, 628–636.
13 H.-P. Fiedler, *Nat. Prod. Lett.*, 1993, **2**, 119–128.
14 J. B. Laursen and Nielsen, *Chem. Rev.*, 2004, **104**, 1663–1685.
15 J. W. Blunt and M. H. G. Munro, *MarinLit, vpc14.7*, Canterbury, New Zealand, 2009.
16 E. Pretsch, P. Bühlmann and C. Affolter, ^{13}C NMR Spectroscopy, in *Structure Determination of Organic Compounds*, Springer-Verlag, Berlin Heidelberg, Germany, 2000, pp 71.160.
17 S. A. Shaw, P. Aleman and E. Vedejs, *J. Am. Chem. Soc.*, 2003, **125**, 13368–13369.
18 F. Neese, *ORCA–an ab initio, Density Functional and Semiempirical program package, Version 2.5*, University of Bonn, 2006.
19 J. P. Perdew, K. Burke and M. Ernzerhof, *Phys. Rev. Lett.*, 1996, **77**, 3865.
20 A. Schafer, H. Horn and R. Ahlrichs, *J. Chem. Phys.*, 1992, **97**, 2571–2577.
21 R. Ahlrichs, personal communication.
22 K. Eichkorn, O. Treutler, H. Ohm, M. Haser and R. Ahlrichs, *Chem. Phys. Lett.*, 1995, **240**, 283–289.
23 K. Eichkorn, F. Weigend, O. Treutler and R. Ahlrichs, *Theoretica Chim. Acta.*, 1997, **97**, 119–124.
24 A. Schafer, A. Klamt, D. Sattel, J. C. W. Lohrenz and F. Eckert, *Phys. Chem. Chem. Phys.*, 2000, **2**, 2187–2193.
25 S. H. Vosko, L. Wilk and M. Nusair, *Can. J. Phys.*, 1980, **58**, 1200–1211.
26 J. Dunning, *J. Chem. Phys.*, 1989, **90**, 1007–1023.
27 J. L. Marshall, *Carbon-Carbon and Carbon-Proton NMR Couplings*, Verlag Chemie International, Deerfield Beach, Florida, 1983.
28 V. Isabelle, F. Robert, M. G. Emile and A. Maurice, *Tetrahedron Lett.*, 2001, **42**, 2669–2671.
29 R. Amira and K. Yoel, *J. Org. Chem.*, 1989, **54**, 5331–5337.
30 D. V. Mavrodi, V. N. Ksenzenko, R. F. Bonsall, R. J. Cook, A. M. Boronin and L. S. Thomashow, *J. Bacteriol.*, 1998, **180**, 2541.
31 L. S. Pierson and L. S. Thomashow, *Mol. Plant-Microbe Interact.*, 1992, **5**, 330.
32 A. Romer and R. B Herbert, *Z. Naturforsch., C: Biosci.*, 1982, **37**, 1070.
33 M. McDonald, D. V. Mavrodi, L. S. Thomashow and H. G. Floss, *J. Am. Chem. Soc.*, 2001, **123**, 9459–9460.
34 J. F. Parsons, K. Calabrese, E. Eisenstein and J. E. Ladner, *Biochemistry*, 2003, **42**, 5684–5693.
35 J. F. Parsons, F. Song, L. Parsons, K. Calabrese, E. Eisenstein and J. E. Ladner, *Biochemistry*, 2004, **43**, 12427–12435.
36 D. V. Mavrodi, R. F. Bonsall, S. M. Delaney, M. J. Soule, G. Phillips and L. S. Thomashow, *J. Bacteriol.*, 2001, **183**, 6454–6465.
37 S. R. Giddens, Y. Feng and H. K. Mahanty, *Mol. Microbiol.*, 2002, **45**, 769–783.
38 C. W. Van't Land, U. Mocek and H. G. Floss, *J. Org. Chem.*, 1993, **58**, 6576–6582.
39 P. R. Buckland, S. P. Gulliford, R. B. Herbert and F. G. Holliman, *J. Chem. Res. Synop.*, 1981, 362.
40 P. R. Buckland, R. B. Herbert and F. G. Holliman, *J. Chem. Res., Synop.*, 1981, 363.
41 C.-G. Kim, A. Kirsching, P. Bergon, Y. Ahn, J. J. Wang, M. Shibuya and H. G. Floss, *J. Am. Chem. Soc.*, 1992, **114**, 4941–4943.
42 T. F. C. Chin-A-Woeng, J. E. Thomas-Oates, B. J. J. Lugtenberg and G. V. Bloemberg, *Mol. Plant-Microbe Interact.*, 2001, **14**, 1006–1015.
43 V. M. Reddy, J. F. O'Sullivan and P. R. Gangadharam, *J. Antimicrob. Chemother.*, 1999, **43**, 615–623.
44 S. Chatterjee, E. K. Vijayakumar, C. M. Franco, R. Maurya, J. Blumbach and B. N. Ganguli, *J. Antibiot.*, 1995, **48**, 1353–1354.
45 M. Muller, *Biochim. Biophys. Acta*, 1995, **1272**, 185–189.
46 W. G. Kim, I. J. Ryoo, B. S. Yun, K. Shin-ya, H. Seto and I. D. Yoo, *J. Antibiot.*, 1999, **52**, 758–761.
47 K. F. Shin-ya, Y. Teshima, Y. Hayakawa and H. Seto, *J. Org. Chem.*, 1993, **58**, 4170–4172.
48 O. G. Pachon, A. Azqueta, M. L. Lavaggi, A. Lopez de Cerain, E. Creppy, A. Collins, H. Cerecetto, M. Gonzalez, J. J. Centelles and M. Cascante, *Chem. Res. Toxicol.*, 2008, **21**, 1578–1585.
49 L. J. Lewis, P. Mistry, P. A. Charlton, H. Thomas and H. M. Coley, *Anti-Cancer Drugs*, 2007, **18**, 139–148.
50 H. J. Lee, J. S. Kim, M. E. Suh, H. J. Park, S. K. Lee, H. K. Rhee, H. J. Kim, E. K. Seo, C. Kim, C. O. Lee, Park and H. Y. Choo, *Eur. J. Med. Chem.*, 2007, **42**, 168–174.
51 D. Li, F. Wang, X. Xiao, X. Zeng, Q. Q. Gu and W. Zhu, *Arch. Pharmacal Res.*, 2007, **30**, 552–555.
52 A. Braca, C. Sortino, M. Politi, I. Morelli and J. Mendez, *J. Ethnopharmacol.*, 2002, **79**, 379–381.
53 T. Yrjönen, L. Peiwu, J. Summanen, A. Hopia and H. Vuorela, *J. Am. Oil Chem. Soc.*, 2003, **80**, 9–14.
54 G. C. Yen and H. Y. Chen, *J. Agric. Food Chem.*, 1995, **43**, 27–37.
55 P. Molyneux, *Songklanakarin J. Sci. Technol.*, 2004, **26**, 211–219.
56 G. Miliauskas, P. R. Venskutonis and T. A. Van Beek, *Food Chem.*, 2004, **85**, 231–237.
57 O. P. Sharma and T. K. Bhat, *Food Chem.*, 2009, **113**, 1202–1205.
58 K. Li, X.-M. Li, N.-Y. Ji and B.-G. Wang, *J. Nat. Prod.*, 2008, **71**, 28–30.

